

# A Rheological Model for Iron Oxide Suspensions

YIH-SHEN LIN, TA-JO LIU\*, and NING-JO CHU

Department of Chemical Engineering, National Tsing Hua University, Hsinchu, Taiwan 30043 ROC

## SYNOPSIS

We have examined the rheological properties of a Co-adsorbed  $\gamma$ -Fe<sub>2</sub>O<sub>3</sub> magnetic suspension with polyurethane (PU) as a binder and methyl ethyl ketone (MEK) or cyclohexanone (CH) as a solvent. A Haake RV20 viscometer was used to measure the suspension viscosity and the vane method was adopted to determine the fluid yield stress. A rheological model which can be viewed as a combination of the Casson model and the Bingham model is proposed to describe the suspension viscosity. The effects of temperature, particle content, and binder concentration are included in the model.

## INTRODUCTION

Recording media such as audio, video, and digital tapes or disks are manufactured by the application of a thin layer of magnetic suspension on various types of substrates. Several coating methods are used to produce recording tapes and disks, and a good understanding of the rheological properties of magnetic suspensions is of great importance for the successful coating operations.

Several authors have investigated the rheological properties of magnetic suspensions. Watanabe<sup>1</sup> measured the time dependence of some rheological properties of a  $\gamma$ -Fe<sub>2</sub>O<sub>3</sub> magnetic paint and studied the structure formation and breakdown of the paint. Smith and Bruce<sup>2</sup> discussed the viscosity of  $\gamma$ -Fe<sub>2</sub>O<sub>3</sub> particles in ethylene glycol. Nagashiro and Tsunoda<sup>3</sup> measured the viscosities of  $\gamma$ -Fe<sub>2</sub>O<sub>3</sub> particles dispersed in epoxy resin, phenolic resin, and poly(vinyl butyral) solutions; the particle content in their study was low and they did not observe any significant fluid yield stress. Yang et al.<sup>4</sup> analyzed the rheological properties of  $\gamma$ -Fe<sub>2</sub>O<sub>3</sub> particles in silicone oil. Huisman<sup>5</sup> and Gooch<sup>6</sup> discussed the dispersion process of a magnetic suspension.

In this paper we shall consider a Co-adsorbed  $\gamma$ -Fe<sub>2</sub>O<sub>3</sub> magnetic suspension with PU as a binder and MEK or CH as a solvent. This system appears to be similar to one of the most popular formulations

for making magnetic tapes and disks. We shall examine the rheological measurements of this suspension system and develop a rheological model to describe the suspension viscosity.

## EXPERIMENTAL

### Materials

The Co-adsorbed  $\gamma$ -Fe<sub>2</sub>O<sub>3</sub> used in our experiments was produced by the Pfizer Co. (Pferico 2560). The average length of the acicular particles is 0.37  $\mu$ m, and the aspect ratio is 6 : 1. The binder PU was obtained from the BF Goodrich Chemical-Europe Co. (Estane 5715).

To prepare a sample suspension for our measurements, we fixed the weight of PU as a basis and varied the weights of Co-adsorbed  $\gamma$ -Fe<sub>2</sub>O<sub>3</sub> particles and solvents. Variations of weight ratio for test materials are given in Table I.

The Co-adsorbed  $\gamma$ -Fe<sub>2</sub>O<sub>3</sub> particles were dried at 120°C for 5 h before use. The PU resin was dissolved in the solvent and then mixed with the particles. A ball mill (type S2, Retsch Co.) was used to prepare the magnetic suspension. Usually 40 h of milling time was required to obtain a well-dispersed test sample.<sup>3</sup>

### Rheological Measurements

A Haake Rotovisco RV20 coaxial cylinder viscometer was selected to measure suspension viscosities

\* To whom correspondence should be addressed.

**Table I** Weight Ratio of Test Materials

Weight Ratio	Material			
	Co-adsorbed $\gamma\text{-Fe}_2\text{O}_3$	PU	CH	MEK
PU/CH System	2.00 ~ 8.20	1	8.6 ~ 15.9	—
PU/MEK System	1.87 ~ 2.72	1	—	5.5

and a MV-1P sensor with grooved surface was used to prevent wall-slip. Viscosity data could be obtained at shear rates ranging from  $0.1 \text{ s}^{-1}$  to  $1000 \text{ s}^{-1}$ . The maximum shear stress for our measurements was 322 Pa.

After a test sample was loaded into the sensor, the sensor was accelerated to the maximum shear rate in 9 min and then remained at that shear rate for 5 min before we started recording the shear stress values. We found that the thixotropic behavior of test samples could be eliminated by this procedure.

Coating operations for magnetic suspensions are usually carried out at room temperature, therefore, the sample temperature was varied in a narrow range, i.e., from  $10^\circ\text{C}$  to  $40^\circ\text{C}$  in our experiments.

Fluids with high solid content generally exhibit a yield stress. There are several methods to estimate the fluid yield stress, and a direct extrapolation from low-shear-rate data is frequently used.<sup>7</sup> However, data at low shear rate may not be reliable and a direct extrapolation could lead to erroneous results. Dzuy and Boger<sup>7</sup> proposed a simple vane method to measure the fluid yield stress directly. They assumed that the vane behaves like a rotating cylinder but without any slip problem at low shear rate. A vane with several blades is inserted into a test sample and rotates. The torque required to rotate the vane is recorded as a function of time. Usually the torque will go up first and reaches a maximum value, then it will fall and approaches a constant value. The fluid yield stress can be determined from the maximum torque as follows

$$Tm = \tau_o \pi d^3 (H/d + 1/3)/2 \quad (1)$$

where  $Tm$  is the maximum torque,  $\tau_o$  is the fluid yield stress,  $d$  and  $H$  are the diameter and height of the vane, respectively. Dzuy and Boger found that the yield stress determined by the vane method was independent of the vane geometry. We built two vanes for our experiments, the first one has four blades and is 4-cm long, the second one has six

blades and is 5-cm long, the diameter of both vanes is 2 cm.

## RESULTS AND DISCUSSION

### Solution Viscosity

The viscosities of PU/solvent mixtures were measured by the Haake RV20 viscometer before adding the  $\gamma\text{-Fe}_2\text{O}_3$  particles into the solutions. Johnson et al.<sup>8</sup> found that the viscosity of polymer solution could be described as follows

$$\eta_s = KC^m \quad (2)$$

here  $\eta_s$  is the solution viscosity,  $C$  is the concentration of polymer resin in the solution,  $K$  and  $m$  are constants. Figures 1 and 2 show the viscosities of PU/CH and PU/MEK systems at three temperatures, respectively. It is clear that the solution viscosities can be represented by eq. (2). We could modify eq. (2) to include the temperature effects; the viscosity functions of the two systems can be described through a least-square fitting procedure by the following equations.

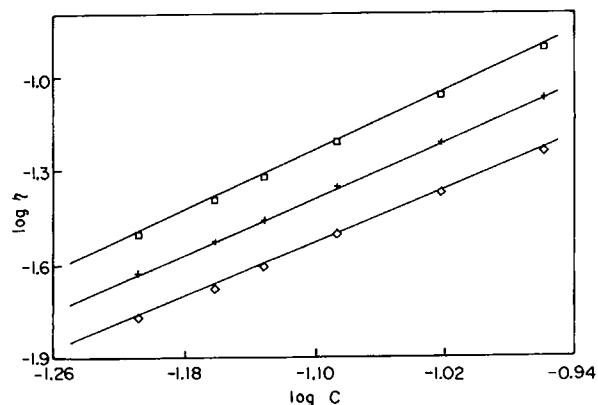


**Figure 1** Solution viscosities  $\eta_s$  ( $\text{Pa}\cdot\text{s}$ ) as a function of PU concentration  $C$  ( $\text{g-PU/g-solution}$ ) for the PU/CH system. ( $\square$ )  $10^\circ\text{C}$ ; ( $+$ )  $25^\circ\text{C}$ ; ( $\diamond$ )  $40^\circ\text{C}$ .

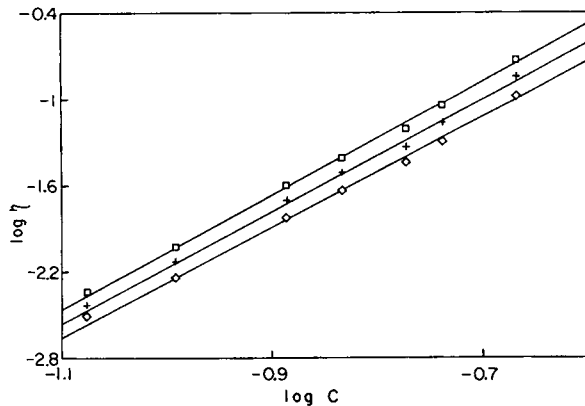


**Figure 2** Solution viscosities  $\eta_s$  (Pa · s) as a function of PU concentration  $C$  (g-PU/g-solution) for the PU/MEK system. ( $\square$ ) 10°C; (+) 25°C; ( $\diamond$ ) 40°C.

### PU/CH System

$$\eta_s = 3.78 \times 10^{-5} C^{(703/T-0.113)} e^{3772/T} \quad (3)$$

### PU/MEK System

$$\eta_s = 2.67 \times 10^{-2} C^{(359/T+2.694)} e^{2262/T} \quad (4)$$

note here  $\eta_s$ ,  $C$ ,  $T$ , and all the remaining variables follow the standard SI units.

### Yield Stress Measurement

The suspension yield stress was measured directly by the vane method. The vane we built was attached to the Hake RV20 viscometer and torque values required to rotate the vane could be recorded. After a vane was inserted into the magnetic suspension, we let it rotate at a high speed for several minutes and then stopped the rotation for a certain time interval before we started performing the yield stress measurements. This procedure is necessary for us to avoid the thixotropic behavior of the suspension and obtain a homogeneous dispersion. Detailed operating procedure can be found elsewhere.<sup>9</sup> Dzuy and Boger<sup>7</sup> stated that the rotational speed of the vane and the vane geometry had little effect on the yield stress measurements. The experimental results of using the four-blade vane for a test sample are given in Table II. When we increased the time interval at a fixed rotational speed or increased the rotational speed, the yield stress measured would increase slightly. Examining the experimental results of Dzuy and Boger, we observed that the yield stress values also increased as the rotational speed increased. The yield stress measurements were repeated with the

**Table II** The Yield Stress Values With CH = 8.6, Co-adsorbed  $\gamma$ -Fe<sub>2</sub>O<sub>3</sub> = 4.4, and PU = 1 (Weight Ratio)

Time Interval	Vane Speed (rpm)				
	0.05	0.083	0.14	0.23	0.39
5 sec	44.7	45.6	45.6	47.2	48.1
20 sec	45.6	46.4	47.2	48.1	48.1
180 sec	48.1	48.1	49.7	49.7	50.5

six-blade vane and we found the results were very close to those of using the four-blade vane. This seems to confirm that the vane geometry has no effect on the yield stress measurements. Even the experimental results of yield stress measurements are somewhat scattered, the differences are generally within 10%. We also estimated the yield stress of the same sample by a direct extrapolation from the low-shear-rate data, the value we obtained was 42 Pa, which is slightly lower than the values in Table II. Therefore, the vane method still can be considered as a reliable means for yield stress measurements. The experimental results shown in Figure 3 indicate that the yield stress increases slightly as fluid temperature rises. However, in our range of measurements, the yield stress can be considered independent of temperature variations.

### Suspension Viscosity and the Rheological Model

Two models are generally used to describe the viscosities of fluids with yield stress. The viscosity expressions for these two models are given as follows

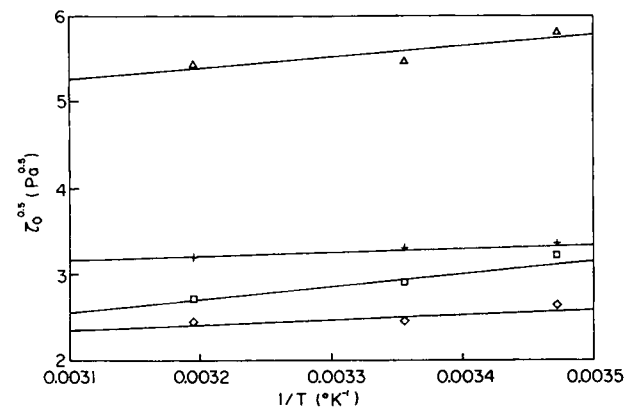


**Figure 3** Temperature dependence of the fluid yield stress. Weight ratio: ( $\Delta$ ) PU/CH/ $\gamma$ -Fe<sub>2</sub>O<sub>3</sub> = 1/8.6/3.0; (+) PU/CH/ $\gamma$ -Fe<sub>2</sub>O<sub>3</sub> = 1/15.9/5.32; ( $\square$ ) PU/CH/ $\gamma$ -Fe<sub>2</sub>O<sub>3</sub> = 1/12.8/4.26; ( $\diamond$ ) PU/MEK/ $\gamma$ -Fe<sub>2</sub>O<sub>3</sub> = 1/5.5/1.87.

**The Bingham Model**

$$\tau = \tau_o + \mu_b \dot{\gamma} \tag{5}$$

here  $\tau$  is the shear stress,  $\dot{\gamma}$  is the shear rate, and  $\mu_b$  is a material constant.

**The Casson Model**

$$\tau^{1/2} = \tau_o^{1/2} + \mu_c^{1/2} \dot{\gamma}^{1/2} \tag{6}$$

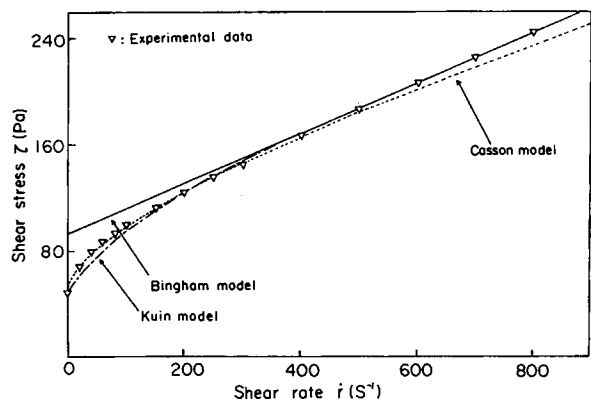
here  $\mu_c$  is a material constant.

Figure 4 shows some of our typical experimental values of a test sample and the best-fitted results of these two models. It is clear that the Casson model is suitable to represent the data at low shear rate, whereas the Bingham model fits the data at high shear rate very well. However, neither model can cover both low-shear-rate and high-shear-rate regions. Recently, a modified Bingham model was proposed to account for low-shear-rate variations of a magnetic dispersion and the modified model is given as

$$\tau = \tau_o + \mu_b \dot{\gamma} - a \cdot \exp(-b\dot{\gamma}) \tag{7}$$

where  $a$  and  $b$  are adjustable constants. We found that the correction term in eq. (7) still could not represent our experimental results satisfactorily. A comparison of the results is given in Figure 4.

Since the Casson model is suitable for our low-shear-rate data and the Bingham model fits our high-shear-rate data well, we propose a new model which is a combination of the Casson model and the Bingham model. The new rheological model is given as follows



**Figure 4** Comparison of three model predictions with the experimental values at 25°C. Weight ratio: PU/CH/ $\gamma$ -Fe<sub>2</sub>O<sub>3</sub> = 1/8.6/4.4.

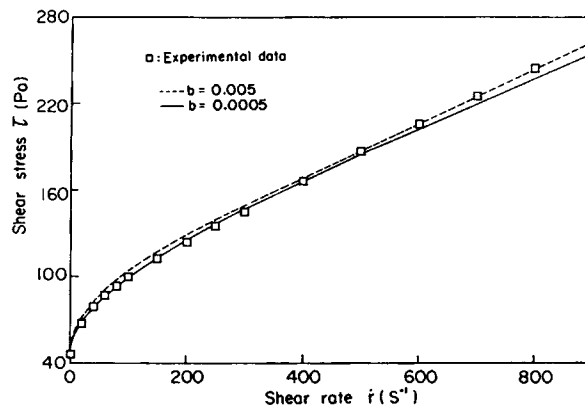


**Figure 5** Variations of  $b$  and comparison with the experimental values at 25°C. Weight ratio: PU/CH/ $\gamma$ -Fe<sub>2</sub>O<sub>3</sub> = 1/8.6/4.4

$$\tau = \{ \tau_o^{1/2} + \mu_c^{1/2} \dot{\gamma}^{1/2} \}^2 \exp(-b\dot{\gamma}) + \{ \tau_b + \mu_b \dot{\gamma} \} [1 - \exp(-b\dot{\gamma})] \tag{8}$$

where  $b$  is an adjustable constant, as  $\dot{\gamma}$  is small, eq. (8) is similar to the Casson model, as  $\dot{\gamma}$  increases, eq. (8) approaches the Bingham model. It should be noted that  $\tau_o$  in eq. (8) is determined directly from the yield stress measurements,  $\mu_c$  is obtained by a least-square procedure using low-shear-rate data, whereas  $\tau_b$  and  $\mu_b$  are obtained using high-shear-rate data through a least-square procedure.  $\tau_b$  in eq. (8) is no longer the true yield stress, it can be viewed as an equivalent Bingham yield value.

It is worth noting that even  $b$  appears as an adjustable constant in eq. (8), varying  $b$  will have little effect on the model predictions. Figure 5 compares the experimental results for  $b = 0.005$  and  $b = 0.0005$ , it is clear that the differences are not significant. Therefore, we fix  $b$  to be 0.005 in our rheological model.

Thomas<sup>10</sup> discussed the relationship between the fluid yield stress and the particle content and developed the following equation

$$\tau_o = \alpha \Phi^\beta \tag{9}$$

where  $\Phi$  is the volume fraction,  $\alpha$  and  $\beta$  are constants, Thomas selected the value of  $\beta$  to be 3 in his work.

As we discussed before, the fluid yield stress we obtained by the vane method varied slightly with temperature and could be assumed to be independent of temperature within the range of our measurements. We found that our experimental results were in agreement with the prediction of eq. (9). Figures 6 and 7 present the values of  $\tau_o$  and  $\tau_b$  as functions of  $\Phi$ , respectively. The slope of the straight lines in

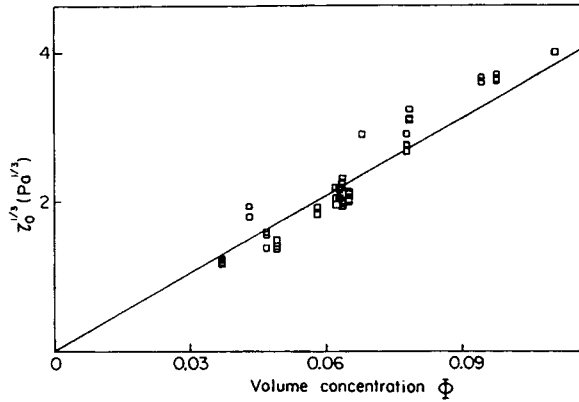


**Figure 6**  $\tau_0$  as a function of Co-adsorbed  $\gamma\text{-Fe}_2\text{O}_3$  volume concentration  $\Phi$  at 25°C.

both figures is 3. Using a least-square fit,  $\tau_0$  and  $\tau_b$  can be expressed as follows

$$\tau_0 = 3.6 \times 10^5 \Phi^{3.8} \quad (10)$$

and

$$\tau_b = 3.47 \times 10^4 \Phi^{2.6} \quad (11)$$

Merrill et al.<sup>11</sup> examined  $\mu_c$  in the Casson model and found it was in proportion to the solution viscosity  $\eta_s$ . We checked the values of  $(\mu_c/\eta_s)$  and found the temperature effects could be excluded without significant errors. Values of  $(\mu_c/\eta_s)^{0.5}$  are shown as functions of solution concentrations in Figure 8. Considering experimental errors, we assumed the following equation was valid

$$(\mu_c/\eta_s)^{0.5} = 1.05 \quad (12)$$

and the errors were within 10%.

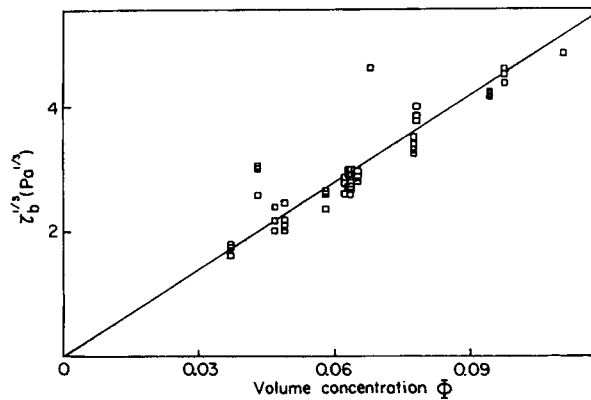


**Figure 7**  $\tau_b$  as a function of Co-adsorbed  $\gamma\text{-Fe}_2\text{O}_3$  volume concentration  $\Phi$  at 25°C.

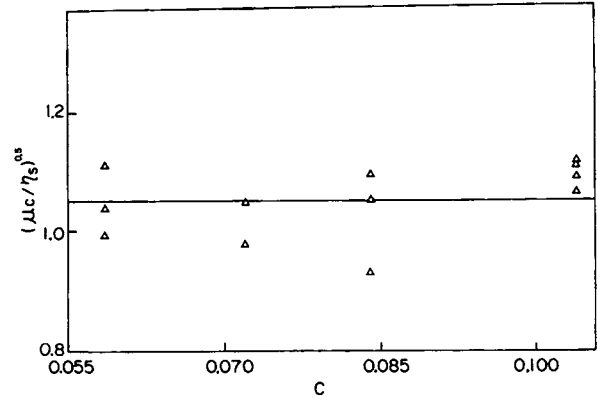


**Figure 8** Variations of  $(\mu_c/\eta_s)^{0.5}$  as a function of PU concentration  $C$  (g-PU/g-solution) at 25°C.

Thomas<sup>10</sup> predicted that  $\mu_b$  in the Bingham model could be expressed as

$$(\mu_b/\eta_s) = \exp(f \Phi) \quad (13)$$

where  $f$  is a constant.

We found that the temperature effects could also be excluded from the ratio of  $\mu_b$  over  $\eta_s$ . Values of  $(\mu_b/\eta_s)$  as functions of  $\Phi$  are shown in Figure 9, using a least-square fit, we obtained

$$\mu_b/\eta_s = 1.02 \exp(9.366\Phi) \quad (14)$$

This equation is in good agreement with Thomas' prediction.

Collecting all the results, we have developed a rheological model that can describe the viscosities of the magnetic suspensions we studied

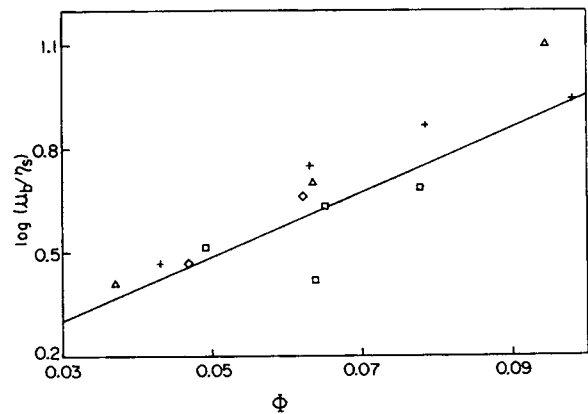


**Figure 9** Variations of  $\log(\mu_b/\eta_s)$  as a function of Co-adsorbed  $\gamma\text{-Fe}_2\text{O}_3$  volume concentration  $\Phi$  at 25°C. ( $\square$ )  $C = 0.104$ ; (+)  $C = 0.084$ ; ( $\diamond$ )  $C = 0.072$ ; ( $\Delta$ )  $C = 0.059$ .

$$\tau = \{\tau_o^{1/2} + \mu_c^{1/2}\dot{\gamma}^{1/2}\}^2 \exp(-0.005\dot{\gamma}) + \{\tau_b + \mu_b\dot{\gamma}\} [1 - \exp(-0.005\dot{\gamma})] \quad (15a)$$

where

$$\tau_o = 3.6 \times 10^5 \Phi^{3.8} \quad (15b)$$

$$\tau_b = 3.47 \times 10^4 \Phi^{2.6} \quad (15c)$$

and

$$(\mu_c/\eta_s)^{0.5} = 1.05 \quad (15d)$$

$$\mu_b/\eta_s = 1.02 \exp(9.366\Phi) \quad (15e)$$

the solution viscosity  $\eta_s$  is

### The PU/CH System

$$\eta_s = 3.78 \times 10^{-5} C^{(703/T-0.113)} e^{3772/T} \quad (15f)$$

### The PU/MEK System

$$\eta_s = 2.67 \times 10^{-2} C^{(359/T+2.694)} e^{2262/T} \quad (15g)$$

Figures 10 and 11 compare the model predictions with some of the experimental results. Generally speaking, the errors were within 10% in the range of our measurements.

## CONCLUSION

We have examined the rheological properties of a magnetic suspension which consists of Co-adsorbed  $\gamma$ -Fe<sub>2</sub>O<sub>3</sub> particles with PU as a binder and CH or MEK as a solvent. The effects of temperature and

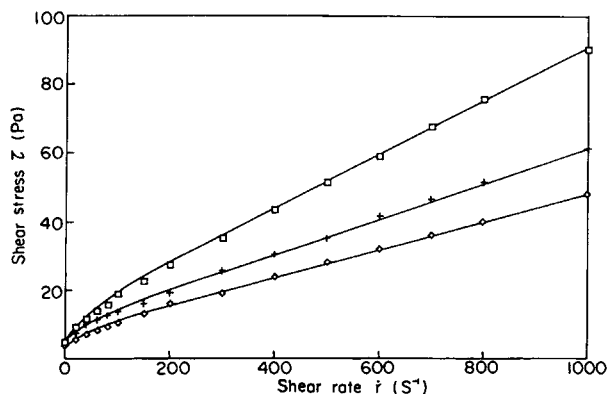


**Figure 10** Comparison of the model prediction eq. (15) with the experimental values. Weight ratio: PU/CH/ $\gamma$ -Fe<sub>2</sub>O<sub>3</sub> = 1/12.8/3.16. (□) 10°C; (+) 25°C; (◇) 40°C.

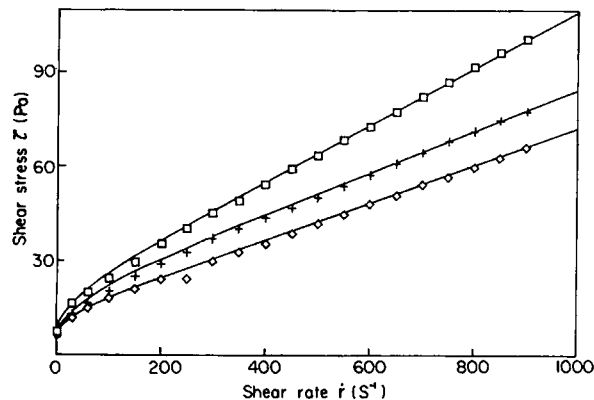


**Figure 11** Comparison of the model prediction eq. (15) with the experimental values. Weight ratio: PU/MEK/ $\gamma$ -Fe<sub>2</sub>O<sub>3</sub> = 1/5.5/1.87. (□) 10°C; (+) 25°C; (◇) 40°C.

composition variations were studied and a rheological model which is a combination of the Casson model and the Bingham model was proposed. This model can adequately describe the rheological properties of the magnetic suspension we studied and the contributions of temperature, particle content, and PU concentration are explicitly included in the model.

This research was supported by the National Research Council, the Republic of China.

## REFERENCES

1. S. Watanabe, Ferrites: *Proc. Int. Cong.*, 1970, Tokyo, Japan, p. 473.
2. T. L. Smith and C. A. Bruce, *J. Colloid Interf. Sci.*, **72**, 13 (1979).
3. W. Nagashiro and T. Tsunoda, *J. Appl. Polym. Sci.*, **25**, 2961 (1980).
4. M. C. Yang, L. E. Scriven, and C. W. Macosko, *J. Rheol.*, **30**, 1015 (1986).
5. H. F. Huisman, *J. Coating Tech.*, **57**, 49 (1985).
6. J. W. Gooch, *J. Coating Tech.*, **60**, 37 (1988).
7. N. Q. Dzuy and D. V. Boger, *J. Rheol.*, **27**, 321 (1983).
8. J. F. Johnson, R. L. LeTourneau, and R. Mattenson, *Anal. Chem.*, **24**, 1505 (1952).
9. Y. S. Lin, MS Thesis, National Tsing Hua University (1989).
10. D. G. Thomas, *AIChE J.*, **7**, 431 (1971).
11. E. W. Merrill, W. G. Margetts, and E. R. Gilliland, *Proceedings of the Fourth International Congress on Rheology*, P. 4, A. L. Copley, Ed., Interscience, New York (1965).

Received September 4, 1989

Accepted June 22, 1990